Mausam, (1989), **40**, 2, 123–130

551.577 : 551.521.14 : 551.507.362

Estimation of precipitation and outgoing longwave radiation from INSAT-1B radiance data

A. V. R. K. RAO & R. R. KELKAR
India Meteorological Department, New Delhi
and
PHILLIP A. ARKIN
Climate Analysis Center, NMC, NOAA, Washington D.C.
(*Received 24 August 1987*)

सार — इस शोध पत्र में इनसेट–1 बी से बाहर जाने वाली दीर्घ तरंग विकिरण तथा मात्रात्मक वर्षण के आकलन करने के लिए उन क्रिया पद्धतियों का विवरण दिया गया है जिन्हें मौसम विज्ञान आंकड़ा उपयोग केन्द्र (MDUC), नई दिल्ली में विकसित किया गया था। इनसेट–1बी के तीन घंटेवार समकक्ष कृष्णिका तापमानों (EBBT) का प्रयोग करते हुए मात्रात्मक वर्षण आकलन (QPE) की प्रक्रिया में एक प्राचल रेखिक निदर्श का प्रयोग किया जाता है। ई. बी. बी. टी. (EBBT) को एक 16-कक्ष आयतचित्र में वितरित किया गया है। चुने हुए प्रभाव सीमा तापमान की अपेक्षा शीत मेघावरण के अभिकलन के द्वारा और उसको समाश्रयण गुणांक के साथ गुणा करके मात्रात्मक वर्षण आकलन (QPE) को परिकलित किया गया है। 40° पूर्व से 100° पूर्व तथा 35° उत्तर से 25° दक्षिण तक फैले एक क्षेत्र में 2.5°×2.5° देशान्तर/अक्षान्तर उपक्षेत्र का अभिकलन किया गया है।

माध्य ताप का प्रयोग करते हुए OLR 2.5° देशांतर/अक्षांतर उपक्षेत्र का अभिलकन किया गया है।

1986 की शीत ऋतु (दिसम्बर 1986 से फरवरी 1987) से संबंधित QPE और OLR के मासिक माध्य चार्ट प्रस्तुत किए गए हैं। OLR के निम्न मान वर्षा क्षेत्रों से अच्छी तरह से मेल खाते हैं। वर्षा क्षेत्र को निरूपित करने के लिए 240 वाटस्/मीटर^2 की समान रेखा पाई गई है।

1987 के जनवरी–फरवरी के दौरान बंगाल की खाड़ी में भीषण चक्रवातीय तूफान के पूर्ण समय का OLR और QPE के दैनिक अभिकलन किए गए। भारी वर्षा के क्षेत्र और निम्न OLR एक समान हैं।

अन्ततः इनसेट OLR मानों की तुलना NOAA के आंकड़ों से की गई है। जबकि उनके बीच प्रतिमान सहसंबंध .85 हैं, अपेक्षाकृत अधिक गर्म क्षेत्रों में NOAA के OLR मान उच्चतर पाए गए हैं।

ABSTRACT. In this paper, methodologies which were developed at Meteorological Data Utilisation Centre, New Delhi, to compute Quantitative Precipitation Estimates (QPE) and Outgoing Longwave Radiation (OLR) from INSAT-1B radiance data, are described. QPE computation employs a one-parameter linear model using 3-hourly INSAT-1B Equivalent Black Body Temperatures (EBBT). The EBBT's are distributed over a 16-class histogram. QPE is computed from the histogram data by calculating fractional cloud cover colder than a chosen threshold temperature and multiplying the same with a regression coefficient. Computations are carried over 2.5° × 2.5° Lat./Long. boxes in an area extending from 40° E to 100°E and 35°N to 25° S.

OLR is computed, using the mean tempertaure of the 2.5° Lat./Long. box.

Monthly mean charts of QPE and OLR are presented for the winter season of 1986 (December 1986 to February 1987). Low values of OLR coincide well with the raining areas. The isopleth of 240 watts/m^2 is found to delineate the raining area.

Daily computation of OLR and QPE were also carried out during the life period of a severe cyclonic storm in the Bay of Bengal during January-February 1987. Areas of heavy rain and low OLR are in agreement.

Finally, INSAT OLR values are compared with those of NOAA. While the pattern correlation between them is .85, OLR values of NOAA are found to be higher in the warmer areas.

1. Introduction

Large-scale precipitation values are of importance in many fields like hydrology, agriculture, climatology and numerical modelling. Anomalies in large-scale precipitation are also known to have a close relationship with global circulation anomalies. Estimation of areal average precipitation from raingauge measurements is, however, subject to several types of errors. These arise from the non-representativeness of point-rainfall measurements, sparseness of the raingauge network and its complete non-existence over oceanic and inaccessible areas, effects of terrain and inherent inaccuracy of the observations. An effective alternative is provided by the digital radar, but its deployment is impracticable over the ocean and it would be prohibitively expensive to have a large radar network on land.

In order to obviate the difficulties of land-based observing systems, many investigators have attempted the estimation of rainfall indirectly from satellite observations of clouds. A review of different techniques employed for this purpose is given by Barrett and Martin (1981). Most satellite-based techniques are built on the hypothesis that brighter (colder) clouds in visible (infrared) imagery are associated with higher precipitation. Such techniques are valid mainly in the tropics, where convective activity is the chief source of

precipitation. Furthermore, satellite methods require the specification of an empirically derived rain rate obtained by comparison with raingauges or radar.

Satellite rain estimation techniques can be classified into two broad categories, *viz.*, (i) estimation of precipitation on near real-time, *e.g.*, Scofield and Oliver (1977), Griffith *et al.* (1978) and (*ii*) estimation of average preciptitation over a large area for a period of time ranging from a day to a month, *e.g.*, Barrett (1970), Kilonsky and Ramage (1976), Richards and Arkin (1981). Since polar-orbiting satellites take only two observations per day over the tropics, methods employing geostationary satellite data have certain obvious advantages.

No systematic quantitative estimates of rainfall based on satellite data are available for the Indian region. However, attempts in this direction have been made by Krishnamurti *et al.* (1983), Martin and Howland (1986) and Bhandari *et al.* (1987) with data from the GOES satellite which was specially positioned over the Indian Ocean during the short period of the Summer Monex.

With the data now flowing from India's own satellite, INSAT-1B, it has become possible for the first time to undertake large-scale precipitation estimation on a regular basis at the Meteorological Data Utilisation Centre, New Delhi. The present paper describes the methodology developed by the authors and discusses some of the early results pertaining to the winter season of December 1986 to February 1987.

Another satellite-derived parameter, *viz.*, the outgoing longwave radiation (OLR), has been found to be well-correlated with rainfall and some attempts have been made to estimate rainfall, given the OLR (Lau and Chan 1983, Arkin *et al.* 1984). OLR also has an important place in earth-atmosphere radiation budget studies (Ohring and Gruber 1983). The present paper includes a description of the technique used by the authors to compute OLR from INSAT-1B infrared radiances and an analysis of the 1986-87 winter season OLR *vis-a-vis* rainfall estimates.

2. Methodology

2.1. *QPE computation procedure*

The method adopted for computing the quantitative precipitation estimate (hereafter abbreviated as QPE) from INSAT-1B infrared data is based on the results of Arkin (1979) and is essentially identical to that described in Arkin and Meisner (1987). The area of analysis extends from 40°E to 100° E and 35° N to 25° S and is divided into 2.5° × 2.5° Lat./Long. boxes. The following steps are involved in the processing :

(*i*) INSAT-1B infrared images of 0000, 0300, 0600, . . . , 2100 UTC, *i.e.*, every three hours, are used. An infrared pixel (picture element) has dimensions of 11×11 km at the subsatellite point, so that several hundred pixels fall within a 2.5°×2.5° box.

(*ii*) The grey shade value (0-255) of each pixel in a given image is read and the corresponding brightness temperature is calculated from a look-up table. Pixels lying outside the chosen area of analysis are ignored by the software while those within it are assigned to the appropriate box. Because of the highly stable orbit and attitude of the INSAT-1B spacecraft, a pixel can be pre-assigned to a box, depending on its position in the image. Bad or missing image lines are eliminated by the software from further processing.

(*iii*) After the temperatures of all the pixels in a box are known they are distributed over a 16-class histogram. There are 12 classes of 5 K interval, *viz.*, 270-266, 265-261, ----------, 215-211 K. After these, there are two classes of 10 K interval, *viz.*, 210-201 and 200-191 K. Two more classes group together all pixels with temperatures exceeding 270 K and those below 190 K respectively.

(*iv*) In addition to the histogram analysis, the mean temperature of each box (sum of the temperatures of all pixels/number of pixels in the box) and the spatial variance of the temperature are also calculated.

(*v*) Steps (*i*) to (*iv*) are repeated for all the 3-hourly images of the day and the daily mean temperature and variance are obtained for each box. The number of pixels in each class of the histogram is summed up over the eight images to get daily accumulated histogram class frequencies for each box.

(*vi*) Step (*v*) is repeated to arrive at histogram accumulation, mean temperature and variance over a given period of time such as pentad, week or month.

(*vii*) The fractional clouding for a box over the chosen period of time is the ratio of the pixels cooler than a specified threshold temperature to the total number of pixels. This gives a measure of the fractional area of the box covered by clouds with tops colder than the threshold.

(*viii*) Finally the quantitative precipitation estimate is obtained from the equation :

$$\mathrm{QPE} = K \times F_c \times N_c \qquad (1)$$

where, F_c is the fractional clouding, K is a constant (in mm/day) related to rain rate, and N_c is the number of days. In the present investigation, the threshold temperature was chosen to be 235 K and a value of 71.2 mm/day was used for the constant K as per Arkin (1979).

2.1.1. *Limitations of the technique*

The methodology outlined above was originally devised for estimation of large-scale rainfall distribution over oceanic areas. Because of the spatial and temporal integration scales involved therein, it may not be suitable for other applications such as short-period forecasting, meso-scale rainfall analysis, etc in which the flattening of rainfall maxima is not desirable. Extension of the technique to land areas may also give unreasonable estimates over mountainous terrain, where the rainfall is primarily orographic and not convective.

The value of the constant K (71.2 mm/day) used here was derived by Arkin (1979) for the GATE area. Like all statistical relationships, this constant is strictly applicable only to the time and location for which it was determined. Revision of this constant for the oceanic areas studied in the present paper, with respect to radar data, is not possible in the absence of the latter,

However, in a separate study, the authors have examined the relationship between QPE and large-scale areal averages of raingauge data over different parts of India during the monsoon season of 1986 (Rao & Kelkar 1987).

The results of this analysis suggest that although the two are well-correlated, the constant K may have to be reduced over some land areas. However, a much wider sample is required before coming to a definite conclusion about the revision of the value of K.

2.2. *OLR derivation procedure*

Satellite estimates of OLR can be made by means of a regression equation between OLR and the narrow-band radiance measurement of the satellite radiometer in the infrared region. In terms of temperature, and for a nadir view, this regression takes the form :

$$T_f = T_r (a + b. T_r) \quad (2)$$

where, T_r is the brightness temperature (in K) measured by the satellite, T_f is the flux temperature (in K), and quantities a and b are constants (Ohring *et al.* 1984). OLR is then computed as σT_f^4 where σ is the Stefan-Boltzmann constant.

The INSAT-1B VHRR (Very High Resolution Radiometer) has an infrared channel operating in the wavelength range of 10.5-12.5μ. Using the spectral response characteristics of this window channel, the constants a and b were evaluated for various zenith angles (Ellingson, private communication). For zero zenith angle, $a = 1.1889$ and $b = 0.000989$/K. With increasing zenith angle, both a and b decrease in magnitude.

For evaluating the constants a and b, radiative transfer calculations are performed on an array of atmospheric profiles to simulate the radiances measured by the satellite radiometer within its wavelength range at different viewing angles.

The computations are repeated for the entire IR range to obtain the total outgoing flux at the top of the atmosphere. The two sets of flux data are then subjected to a regression analysis which yields the values of a and b. The details of the procedure are described by Ellingson and Ferraro (1983) and Ohring *et al.* (1984).

Knowing the brightness temperature of each individual pixel in an INSAT-1B image, the mean OLR of a 2.5°× 2.5° Lat./Long. box can be computed in two ways. One way is to calculate OLR for each pixel by applying Eqn. (2) to its temperature and then to average all the OLR values within the box. Another simpler way is to derive a mean temperature for the box and obtain a single OLR value corresponding to it, neglecting the zenith angle variation within the box. Test computations revealed that the two different approaches lead essentially to the same results. The OLR for the mean temperature differs at the most by 1 to 2 W/m² from the mean OLR for a box. In view of this, the daily OLR was computed from the daily mean box temperature for the purpose of the present study. The daily OLR was averaged over longer periods of time, weeks or months, as needed. In this context, it should be mentioned that Gruber *et al.* (1983), who studied the effect of non-linearity of OLR with respect to temperature with a sample of NOAA-7 data, found differences of the same order.

3. Results and discussion

3.1. *Monthly averages of QPE and OLR*

Figs. 1-2 depict the mean monthly QPE and OLR patterns for the months of December 1986, January 1987 and February 1987 respectively. These are based upon 2.5° × 2.5° Lat./Long. grid point values for the area 40°-100° E, 35°N-25° S. The QPE values are in units of mm/month obtained from monthly accumulation of 3-hourly histograms as explained in section 2.1 above. The monthly OLR values in W/m² are averages of daily OLR which in turn is calculated from daily mean temperature as described in section 2.1.

3.1.1. *QPE patterns*

Of the three winter months (which correspond to southern hemispheric summer months), January is seen to be the wettest. There are three zones of heavy rainfall (>300 mm) in this month, one located over Madagascar, another along 6° S in the west Indian Ocean, and a third near the equator in the east Indian Ocean which is the most pronounced among the three (>400 mm). The heavy rainfall over the ocean could partially be attributed to cyclonic activity over the southern hemisphere in January. However, areas around Madagascar and Indonesia had heavy rainfalls even in December.

The QPE isohyets generally exhibit an east-west orientation except over and near land masses. They also tend to shift southwards as the summer recedes from the southern hemisphere.

In general, rain amounts in the northern hemisphere south of 25° N are insignificant. The rainfall observed over the Bay of Bengal in January and February appears to have been associated with the formation of a cyclonic storm in the last week of January. This aspect is examined in detail in section 3.3.

North of 25°N, winter rain is due to the passage of western disturbances and the relatively higher QPE (100-200 mm in December and February) reflects this activity. However, over the Tibetan plateau, where surface temperatures are themselves very low in winter, the interpretation of the histogram values in terms of fractional clouding may not be always valid. Thus, the higher QPE values (>200 mm) in the winter months on the Tibetan plateau may be overestimates. Moreover, the method of precipitation estimation used in this study has been formulated mainly for the tropical oceanic area, and its direct application to the land areas of higher latitudes may not yield accurate results (Arkin and Meisner 1987).

3.1.2. *OLR analysis*

OLR isopleths in the winter months are characterised by a predominantly latitudinal orientation. The lowest values of OLR (< 180 W/m²) are observed over the Tibetan plateau, increasing sharply southwards across the Himalayas. The OLR "high" (> 260 W/m²) lies along 15° N latitude in all the three months.

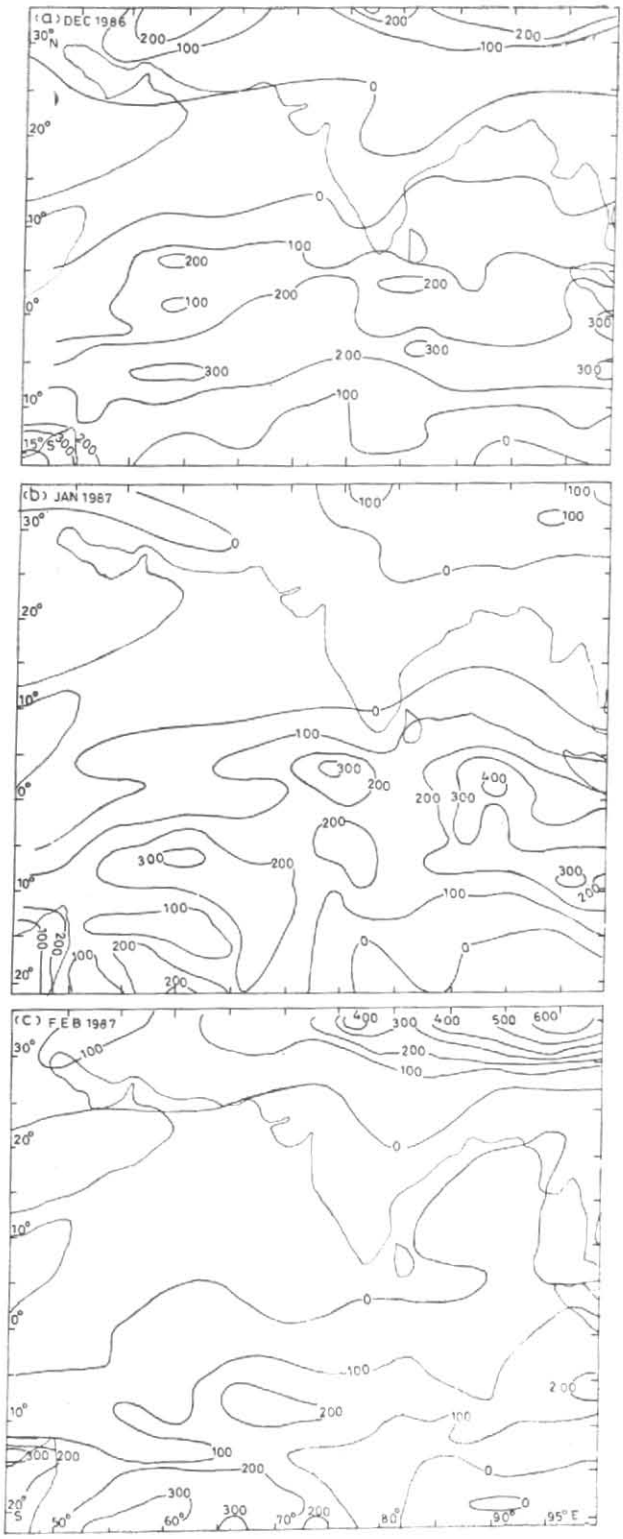

Figs. 1(a-c). Isopleths of QPE (in mm/month) for (a) December 1986, (b) January 1987 and (c) February 1987

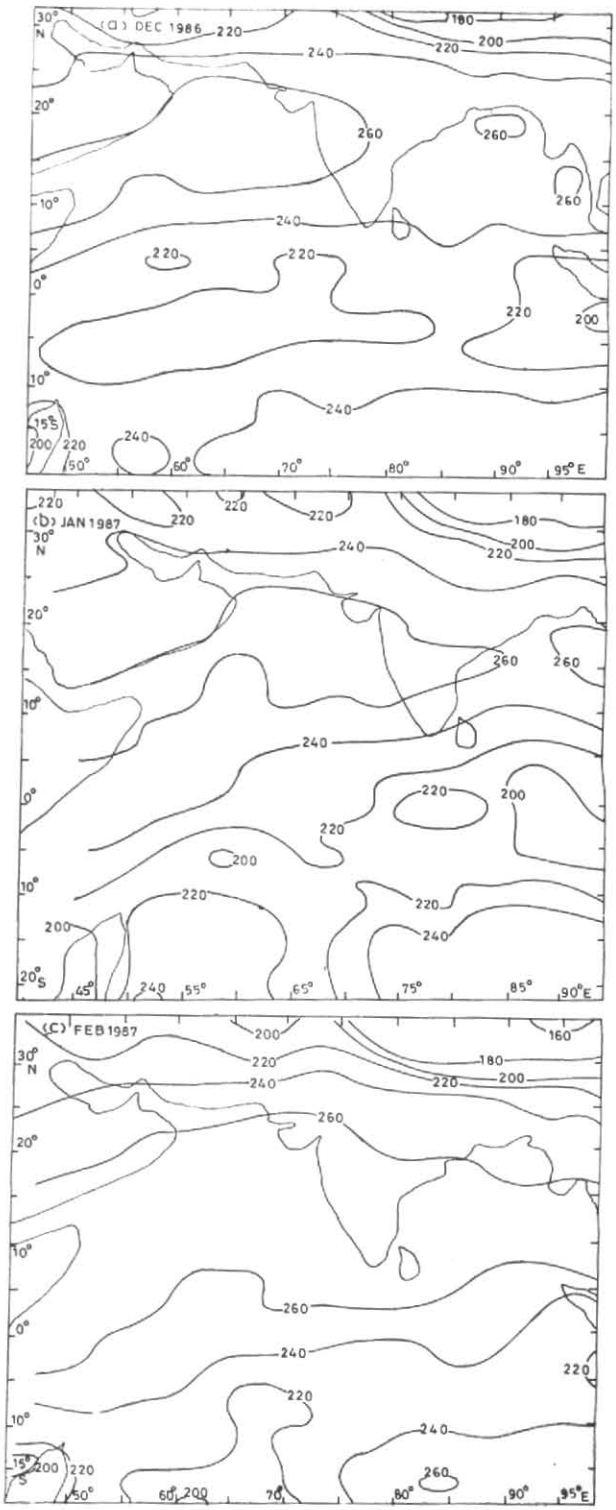

Figs. 2(a-c). Isopleths of mean OLR (in W/m²) for (a) December 1986, (b) January 1987 and (c) February 1987

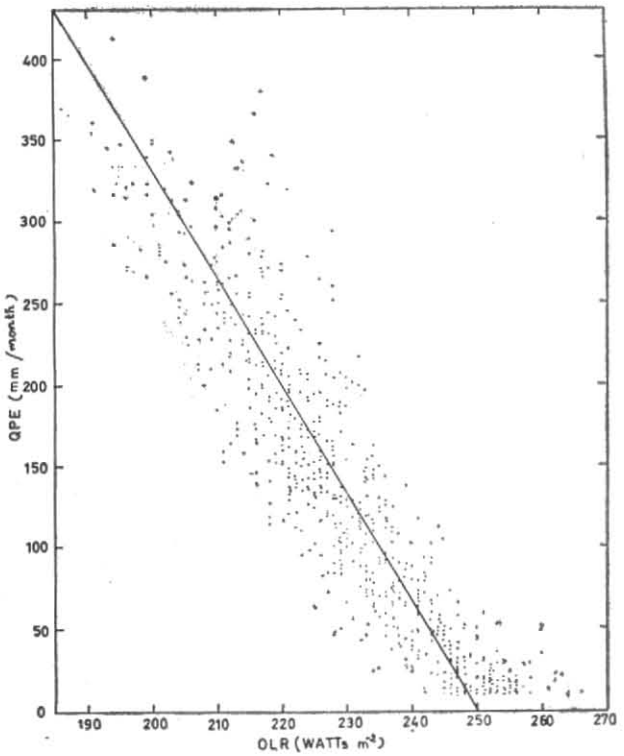

Fig. 3. Scatter diagram of monthly QPE against OLR for December 1986 to February 1987 for oceanic grid-points over the area of study

In the southern hemisphere, OLR values are lowest in January, implying increased convective activity in that month. There is a secondary OLR high in the southeast Indian Ocean area throughout the southern summer. Between the two OLR highs, the values range from 200 to 240 W/m². This belt of low values, however, is seen to shift southwards from December to February.

3.2. *Relationship between QPE and OLR*

In the tropics, where large-scale precipitation is mainly from convective clouds, it is reasonable to expect that OLR, which is an index of convective activity, would be related inversely to the rainfall amounts. This hypothesis appears to be borne out in the investigations of Arkin (1984) and Morrissey (1986).

Arkin's work was based upon twice-daily OLR of NOAA satellites spatially averaged over 2.5°×2.5° Lat./Long. boxes and over temporal scales of month, seasons and year, which was compared with rainfall data of island stations in the Pacific. Arkin found that the mean OLR and total observed rainfall were linearly related and so were their anomalies.

Morrissey's investigation was done with daily NOAA OLR averages over 3.75°×3.75° Lat./Long. squares as compared with station rainfall data over Australia and Pacific Ocean islands. He found a correlation coefficient of —0.52 which was statistically singnificant but the scatter was large in both variables due to local effects in rainfall measurements and "cirrus contamination" of OLR.

In the present work, a comparison of monthly patterns of QPE (Fig. 1) and OLR (Fig. 2) confirm the inverse relationship between the two parameters. Low OLR values coincide with areas of heavy QPE and OLR highs correspond to the dry areas. The orientation of the isopleths of both the parameters is similar in each of the three winter months. Generally speaking the 240 W/m² OLR isopleth delineates the areas of appreciable rainfall on a monthly scale. However, if monthly QPE-OLR pairs are plotted on a scatter diagram (Fig. 3) the threshold of OLR demarcating raining and non-raining areas is found to be 250 W/m² on the average. Fig. 3 is based on data over the oceanic areas only. Construction of a scatter diagram for land points was not possible because of paucity of data.

It is known that convective clusters in the tropical areas develop large mesoscale anvils. Thus, in Fig. 3 QPE and OLR do not have one to one correspondence indicating that although OLR is an index of convective activity all QPE does not come from convective clouds.

3.3. *Case study of a cyclonic storm*

The winter season is normally free from cyclonic activity in the Indian seas. However, during January-February 1987, there was a rare occurrence of a severe cyclonic storm over the Bay of Bengal.

3.3.1. *Synoptic situation*

Starting as a low-pressure trough over southeast Bay of Bengal on 29 January 1987, the system rapidly concentrated into a depression the next day with centre at 6°N,89°E. Initially it moved northwestwards and intensified into a cyclonic storm centred near 8° N, 86° E on the evening of 31 January. Then it started recurving and further intensified into a severe cyclonic storm with a core of hurricane winds centred near 9.5° N, 86° E at 12 UTC of 1 February. The system moved thereafter in a northeasterly direction and was centred near 16.5° N, 91° E at 00 UTC of 3 February. At 09UTC of the same day it started weakening into a cyclonic storm and became a deep depression at 03 UTC of 4 February, with centre near 20°N, 91°E. The storm weakened further and became a low-pressure area at 12 UTC of the same day. It crossed the Bangladesh coast between Cox's Bazaar and Chittagong on the night of 4 February. The storm track is shown in Fig. 4.

3.3.2. *Daily OLR and QPE in relation to storm movement*

The daily OLR and QPE analysis over the Bay of Bengal area from 28 January to 3 February 1987 is shown in Figs. 5 (a-g) respectively. For each figure, 3-hourly INSAT images from 06 UTC of date to 03 UTC of subsequent date have been used in the derivation of mean OLR and daily QPE as per the methods described in sections 2.1 and 2.2.

A comparison of the day-to-day patterns of OLR and QPE reveals that, by and large, the 240 W/m² isopleth demarcates the raining area. Within the area bounded by this isopleth, QPE is seen to increase as the OLR value decreases. This result is in agreement with Lau and Chan (1983) and Morrissey *et al.* (1986) who also found OLR threshold values 240 W/m² for daily and pentad rainfall.

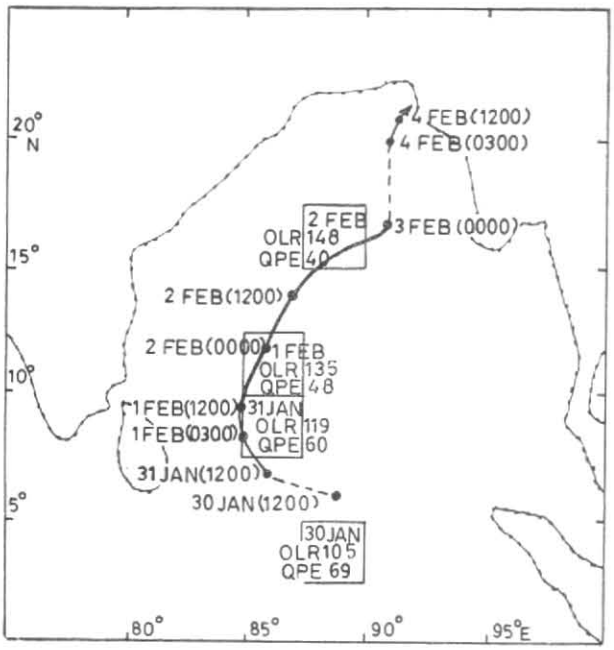

Fig. 4. Track of cyclonic storm. Values within boxes are OLR in W/m² and QPE in mm/day for given date

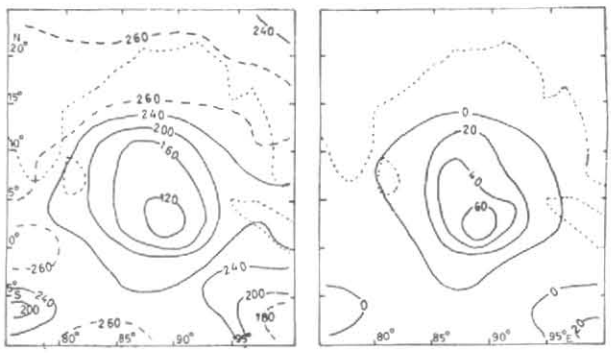

Fig. 5(c). (Left) OLR in W/m² and (right) QPE in mm/day for 30 Jan

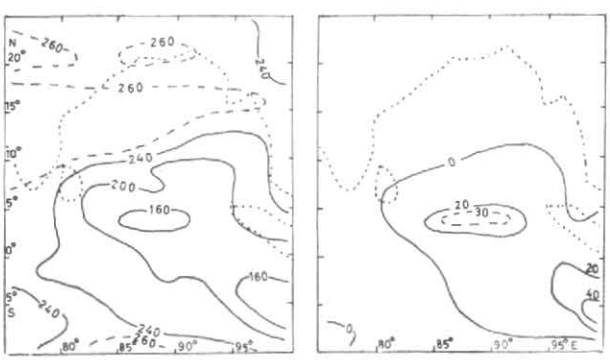

Fig. 5(a). (Left) OLR in W/m² and (right) QPE in mm/day for 28 Jan

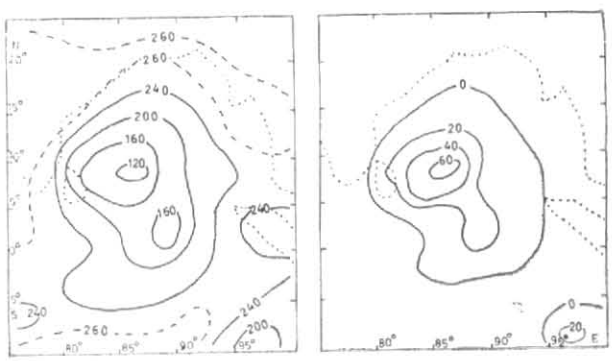

Fig. 5(d). (Left) OLR in W/m² and (right) QPE in mm/day for 31 Jan

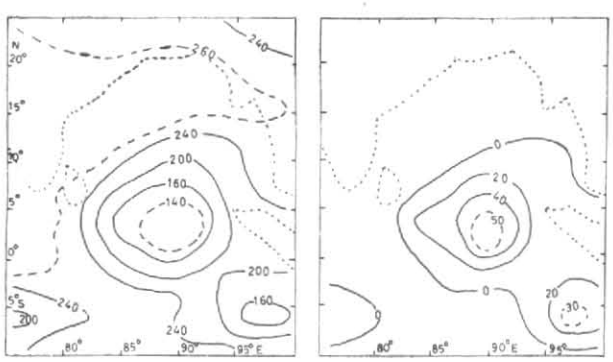

Fig. 5(b). (Left) OLR in W/m² and (right) QPE in mm/day for 29 Jan

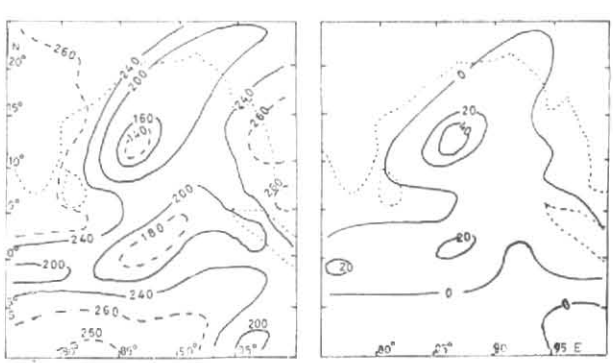

Fig. 5(e). (Left) OLR in W/m² and (right) QPE in mm/day for 1 Feb

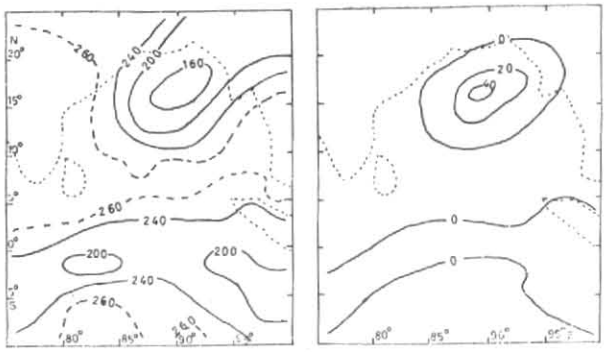

Fig. 5(f). (Left) OLR in W/m² and (right) QPE in mm/day for 2 Feb

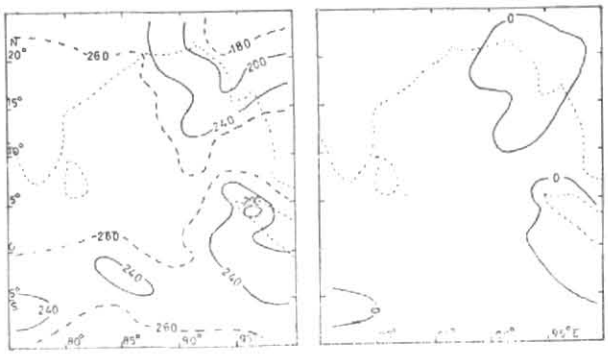

Fig. 5(g). (Left) OLR in W/m² and (right) QPE in mm/day for 3 Feb

The daily OLR and QPE patterns (Figs. 5 a-g) during the 7-day storm period, clearly bring out the developing, mature and decaying stages of the cyclonic storm. On 28 January, there is a zone of maximum QPE and minimum OLR over the extreme southeast Bay of Bengal. On the following day, both the QPE and OLR isopleths are seen to get tightly organised, similar to a pattern of closed isobars. On 30 and 31 January, the minimum OLR zone 120 W/m² corresponds to the maximum QPE area of 60 mm/day. Between 30 and 31 January, there is a clear northwestward movement of this zone. On 1 February, the minimum OLR and QPE zone moved northeastwards and the 240 W/m² OLR isopleth covered almost the entire Bay of Bengal. Here again the raining area closely coincides with the 240 W/m² OLR isopleth. Subsequent patterns bring out the movement towards northeast and absence of closed isopleths as the storm decayed.

The grid boxes in which OLR minimum and QPE maximum occurred are shown over the storm track chart in Fig. 4. They are seen to be in good agreement.

Figs. 5(a-g) are presented to show the correspondence between QPE and OLR patterns on a daily scale. No quantitative relationships are attempted to be established. The qualitative resemblance will be helpful in those situations where OLR data only are available but not QPE, for example with NOAA polar orbitting satellites OLR can be derived but not QPE.

In the case where cyclone development takes place far away from the coast, the indication of the development of the system through the daily averaged OLR changes would give a good lead time to a cyclone forecaster. This can be an additional tool for him to infer about the intensification.

3.3.3. *OLR and QPE as indicators of cyclogenesis*

On three consecutive days, *viz.*, 28, 29 and 30 January, the minimum OLR and maximum QPE were observed over the 2.5°×2.5° box centred at 3.75°N, 88.75°E. Moreover, within this three-day period, OLR in this box decreased progressively from 148 to 105 W/m² while QPE increased from 36 to 69 mm/day. The system was classified as having T. No. 2.5 (representing a cyclonic storm) on 30 January at 06 UTC with centre 5.5°N, 89°E as determined from satellite pictures, which is close to the box mentioned above. The present case study suggests that areas marked by persistent low values of OLR much below the seasonal value should be carefully watched as potential cyclogenetic zones. However, a large number of cyclonic storms must be studied before defining a quantitative threshold of OLR as a pre-indicator of cyclogenesis.

4. Validation of OLR

The monthly averages of OLR over 2.5°× 2.5° Lat./Long. boxes as derived for INSAT-1B temperatures using Eqn. (2) were compared with the corresponding values of OLR obtained from NOAA-9 satellite. The INSAT averages are based on 8 observations a day (0600, 0900,. . ., 0300 UTC), whereas NOAA OLR is an average of only 2 observations a day (0230 and 1430 LT). The resolutions of the two satellites are different (NOAA-1 km and INSAT - 11 km) so also are their viewing angles, spectral widths and their response characteristics. Inspite of these differences, the pattern correlation coefficient between the two sets is 0.97 for the winter season. It is also observed that at an OLR value of about 200 W/m² NOAA and INSAT values are in good agreement, while over warmer regions NOAA values are systematically higher than the INSAT values. This aspect needs further investigation with larger data sets on smaller time scales. This is being analysed and the results will be presented subsequently.

5. Concluding remarks

(*i*) The method of estimating areal average rainfall from satellite radiance data of Arkin (1979) is already being used successfully on an operational mode with US geostationary satellites. Application of this method to INSAT-1B data has now opened up an entirely new approach to the estimation of areal average rainfall over India and adjoining ocean areas. A methodology has also been developed to derive OLR from INSAT- 1B data. These products can now be used in hydrological and agricultural applications and as inputs to numerical model experiments.

(*ii*) The major advantages of satellite-based derivation are the large and contiguous spatial coverage which includes oceanic and inaccessible areas and the availability of the products in near real time. The 24-hour QPE prior to 03 UTC of a given day is available for dissemination by 04 UTC. Conventional rainfall data is absent over the oceans, while the

collection of data from land stations at a central point may take several hours. However, it should be recognised that for certain purposes, data of greater resolution either from raingauge or radar are required and cannot be substituted by satellite estimates.

(*iii*) Conversion of point rainfall to areal averages depends upon the representativeness of the raingauge observation, density of the network over the area and the method of computation itself. As against this, satellite QPE is an areal estimate and hence it is preferable.

(*iv*) In this paper QPE and OLR patterns have been found to have a good resemblance on a daily as well as monthly scale. However, both parameters have been derived from a common source of information, namely, INSAT-1B infrared radiance data. Although the relationship between satellite OLR and raingauge measurements has been established by other authors (Morrissey 1986), it is desirable to undertake such work with the INSAT OLR for Indian area.

Acknowledgements

This work was undertaken as a joint collaborative project under INDO-US Science & Technology Initiative on Monsoon Research. The authors gratefully acknowledge the support received by them from India Meteorological Department, Department of Science & Technology, Government of India and National Science Foundation of U.S.A. Thanks are due to Dr. Robert G. Ellingson, of the Department of Meteorology, University of Maryland for providing the coefficients in the derivation of INSAT OLR . The authors also thank Mrs. Anita Arora and Shri Atiq Ahmed who typed the manuscript and Shri V.P. Bawalia for preparing the diagrams.

References

Arkin, P.A., 1979, The relationship between fractional coverage of high cloud and rainfall accumulations during GATE over the B-Scale array, *Mon. Weath. Rev.*, **107**, pp. 1382-1387.

Arkin, P.A., 1984, An examination of the southern oscillation in the upper tropospheric tropical and subtropical wind field; Ph.D. Thesis, Univ. of Maryland, pp. 223-228.

Arkin, P.A., Janowiak, J.E. and Replane, W., 1984, Large scale variability in Indian monsoon rainfall inferred from satellite data : Proc. Ninth Climate Diagnostics Workshop, Corvallis, NOAA, pp. 265-273.

Arkin, P.A. and Meisner, B.N., 1987, The relationship between large-scale convective rainfall and cold cloud over the Western Hemisphere during 1982-84, *Mon. Weath. Rev.*, **115**, 51-74.

Barrett, E.C., 1970, The estimation of monthly rainfall from satellite data, *Mon. Weath. Rev.*, **98**, 322-327.

Barrett, E.C. and Martin, D.W., 1981, *The use of satellite data in rainfall monitoring*, Academic Press, 340 pp.

Bhandari, S.M., Rao, B.M., Narayanan, M.S., Raghavan, S., Martin, D.W. and Auvine, B., 1987, Rainfall estimation using geostationary satellite VHRR imagery and validation with simultaneous radar rainfall measurements; Scientific Report : ISRO-SAC-SR-27-87, ISRO, Bangalore, 32 pp.

Ellingson, R.G. & Ferraro, R. R., 1983, An examination of a technique for estimating the long wave radiation budget from satellite radiance observations, *J. Clim. appl. Met.*, **22**, 1416-1423.

Griffith, C. C., Woodley, W. L. Grube, P.G., Martin, D. W., Stout, J. and Sikdar, D.N., 1978, Rain estimation from geosynchronous satellite imagery—Visible and Infrared studies, *Mon. Weath. Rev.*, **106**, 1153-1171.

Gruber, A., Ruff, I. and Barnet, C., 1983 Determination of the planetary radiation budget from TIROS-N satellites, NOAA Tech. Rep. NESDIS 3, 12 pp.

Kilonsky, B.J. and Ramage, C.S., 1976, A technique for estimating tropical open ocean rainfall from satellite observations, *J. appl. Met.*, **15**, 972-975.

Krishnamurti, T.N., Cocke, S., Fasch, R. and Low-Nam, S.V., 1983, Precipitation estimates from raingauges and satellite observations; Summer MONEX; Rep. No. 83-7-Deptt. of Met., Florida State Univ., Tallahassee, U.S.A.

Lau, K. and Chan, P.H., 1983, Short-term climate variability and atmospheric teleconnections from satellite observed outgoing longwave radiation. Part-I : Simultaneous relationships, *J. atmos. Sci.*, **40**, 2735-2750.

Martin, D.W. and Howland, M.R., 1986, Grid history : A geostationary satellite technique for estimating daily rainfall in the tropics, *J. Clim. appl. Met.*, **25**, 184-195.

Morrissey, M.L., 1986, A statistical analysis of the relationship among rainfall, outgoing longwave radiation and the moisture budget during January-March 1979, *Mon. Weath. Rev.*, **114**, 931-942.

Ohring, G. and Gruber, A., 1983, Satellite radiation observations and climate theory, *Adv. in Geophysics*, **25**, 237-304.

Ohring, G., Gruber, A. and Ellingson, R., 1984, Satellite determination of the relationship between total longwave radiation flux and infrared window radiance, *J. Clim. appl. Met.*, **23**, 416-425.

Rao, A.V.R.K. and Kelkar, R.R., 1987, Estimation of precipitation from INSAT-1B data, Proc. of National Space Science Symposium, Ahmedabad, Dec. 21-24, 362-364.

Richards, F. and Arkin, P., 1981, On the relationship between satellite observed cloud cover and precipitation, *Mon. Weath. Rev.*, **109**, 1081-1093.

Scofield, R.A. and Oliver, V.J., 1977, A scheme for estimating convective rainfall from satellite imagery, NOAA Tech. Memo., NESS 86, 47 pp.